Supporting Information

Molecular dynamics as an efficient process to predict ^{15}N chemical shift anisotropy at very high NMR magnetic field

*Maggy Hologne[a], Po-Chia Chen[b], François-Xavier Cantrelle[c] and Olivier Walker[a]**

[a]Universite de Lyon, CNRS, UCB Lyon1, Institut des Sciences Analytiques, UMR5280, Villeurbanne, France

[b]School of physics, University of Sydney, Australia

[c]Université de Lille, CNRS, UMR8576 – UGSF – Unité de Glycobiologie Structurale et Fonctionnelle, Lille, France

Figure S1: Theoretical dependence of NMR spin relaxation parameters

(a) Dependence of the NMR spin relaxation parameters R_1, R_2, and NOE as a function of various CSA values and NH vector orientation with respect to the principal axis frame for a ^1H frequency of 600MHz. The synthetic data were obtained by assuming local model-free combined with an axially symmetric molecular reorientation from equations 4-7 of the main text. Typical parameters for restricted local backbone dynamics in the protein core were used with $S^2 = 0.84$, a local motion $\tau_{loc} = 10$ ps, a global tumbling $\tau_c = 5.0$ ns and an anisotropy $D_{\parallel}/D_{\perp}$ of 1.3. (b) Dependence of the NMR spin relaxation parameters R_1, R_2, and NOE as a function of various CSA values in the case of isotropic model for a ^1H frequency of 1200MHz. (c) Dependence of the NMR spin relaxation parameters R_1, R_2, and NOE as a function of various CSA values in the case of isotropic model for a ^1H frequency of 600MHz.

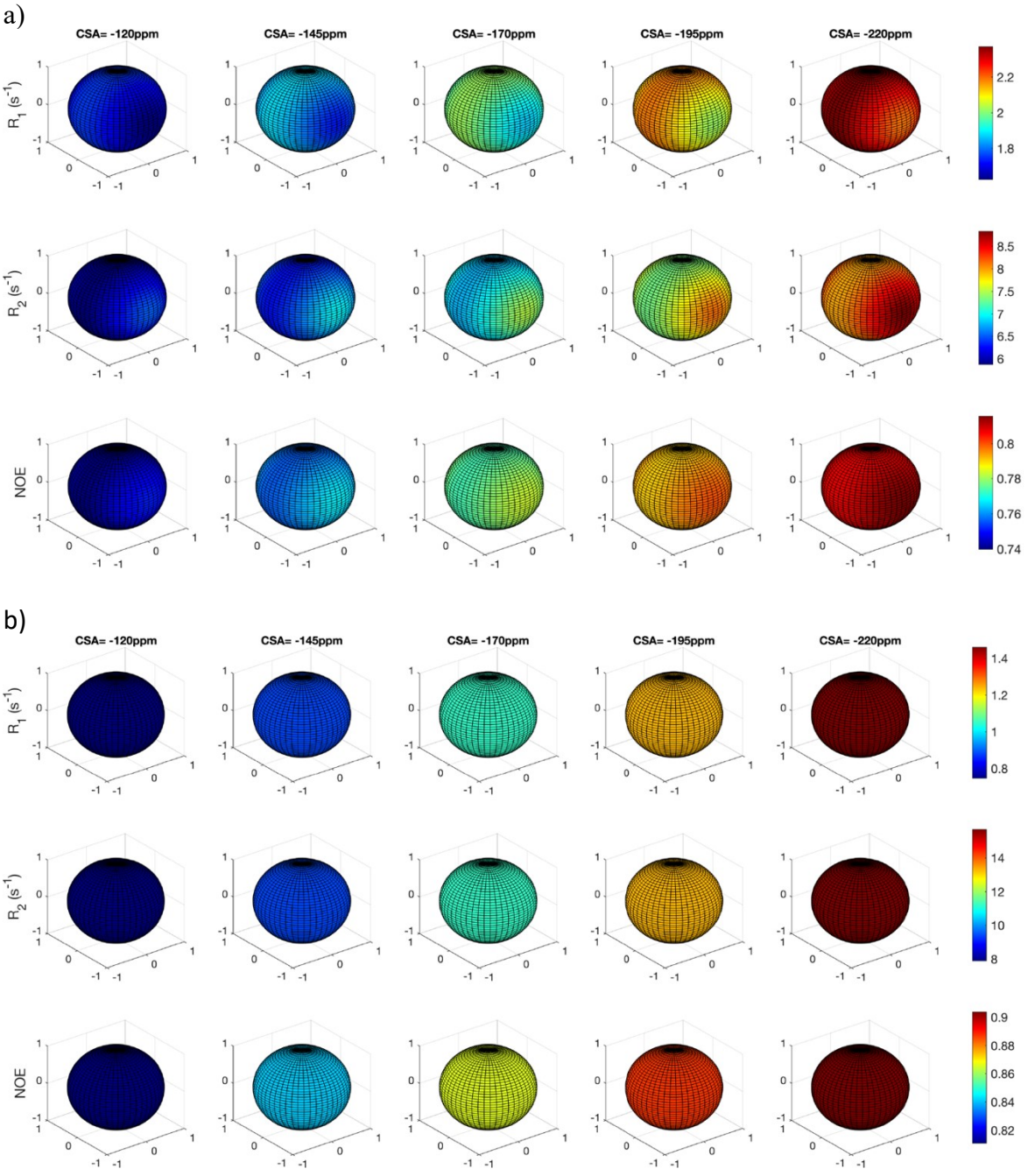

c)

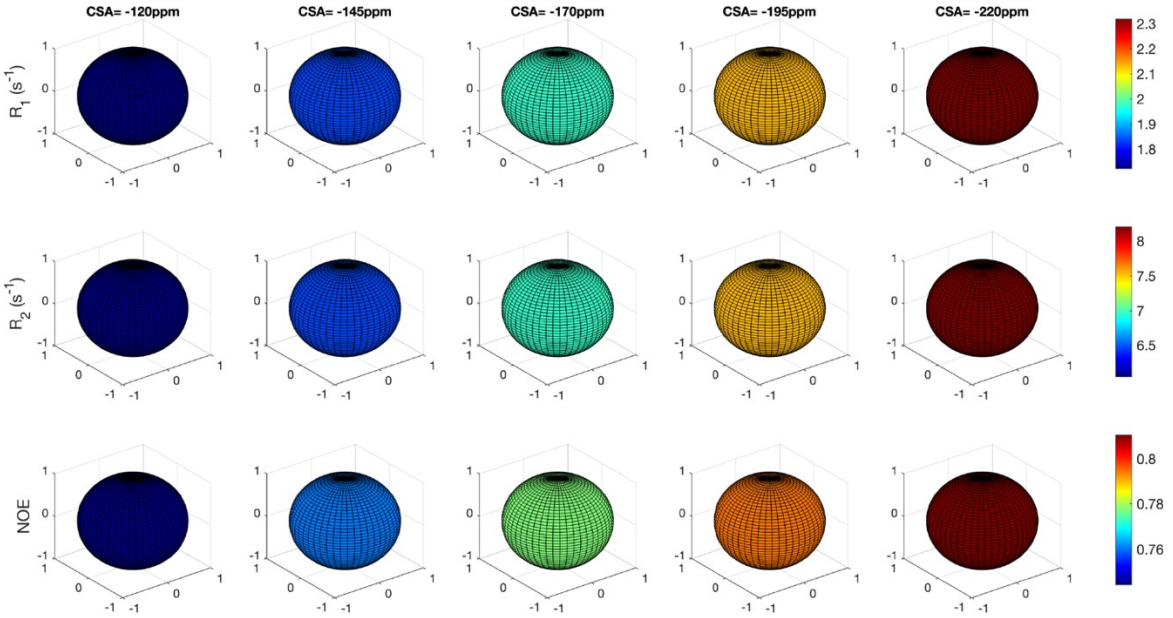

Figure S2: Theoretical dependence of NMR spin relaxation parameters for a high anisotropy

Dependence of the NMR spin relaxation parameters R_1, R_2, and NOE as a function of various CSA values and NH vector orientation with respect to the principal axis frame for a ^1H frequency of 1200MHz. The synthetic data were obtained by assuming local model-free combined with an axially symmetric molecular reorientation from equations 4-7. Typical parameters for restricted local backbone dynamics in the protein core were used with $S^2 = 0.84$, a local motion $\tau_{loc} = 10$ ps, a global tumbling $\tau_c = 5.0$ ns and an anisotropy $D_{\parallel}/D_{\perp}$ of 2.5.

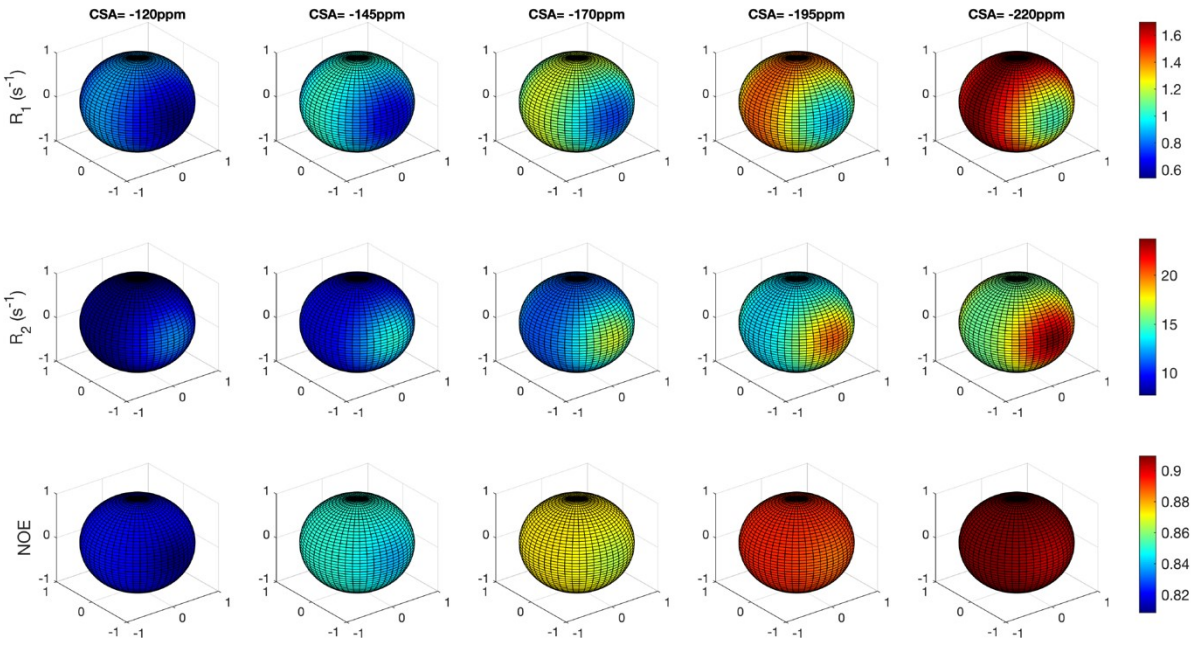

Figure S3: Representation of the different parameters S^2, τ_{loc} and residue-by-residue CSA as a function of residue number.

Each residue is described by 50 randomly oriented NH vectors. S2, τ_{loc} and CSA were sampled according to a gaussian distribution with a mean and standard deviation of 0.85 ± 0.03, 20 ± 5 ps and -170 ± 25 ppm for the S^2, τ_{loc} and CSA respectively. The bottom right panel shows the orientation of the NH vectors with respect to the PAF (in red).

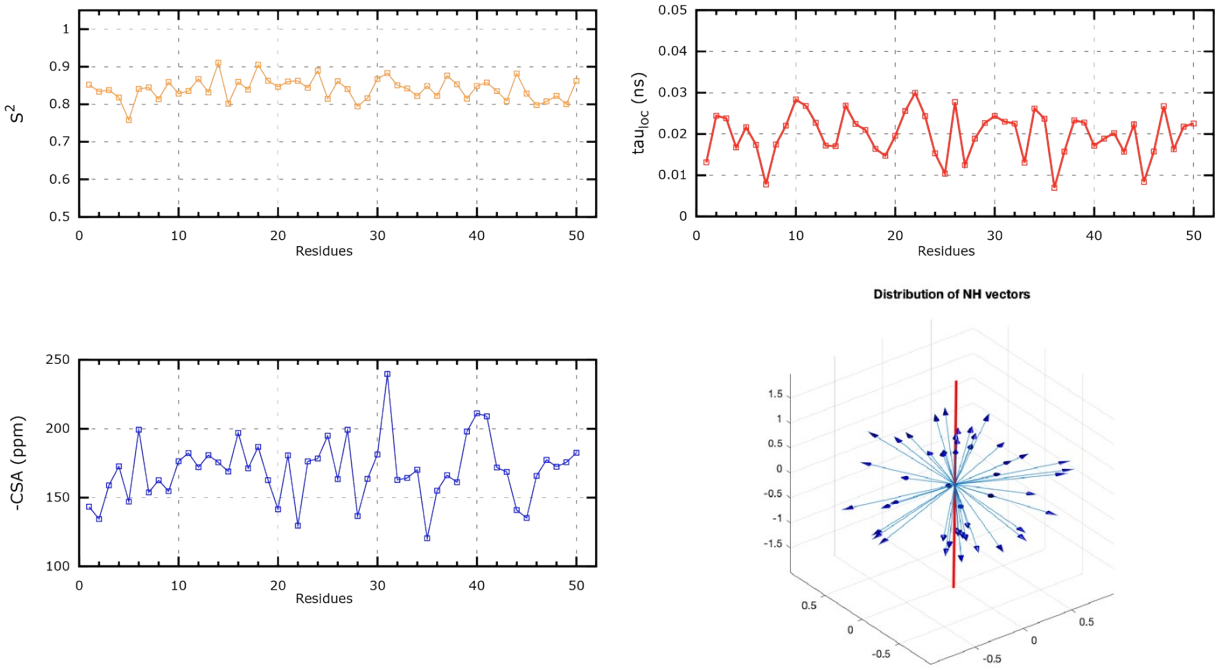

Figure S4: Representation of the synthetic relaxation parameters R_1, R_2 and NOEs.

The parameters are calculated according to the above parameters and for a magnetic field of 9.4 (blue), 14.1 (red), 21.4 (violet) and 28.2 T (green), hence a ^{1}H frequency of 400, 600, 900 and 1200 MHz.

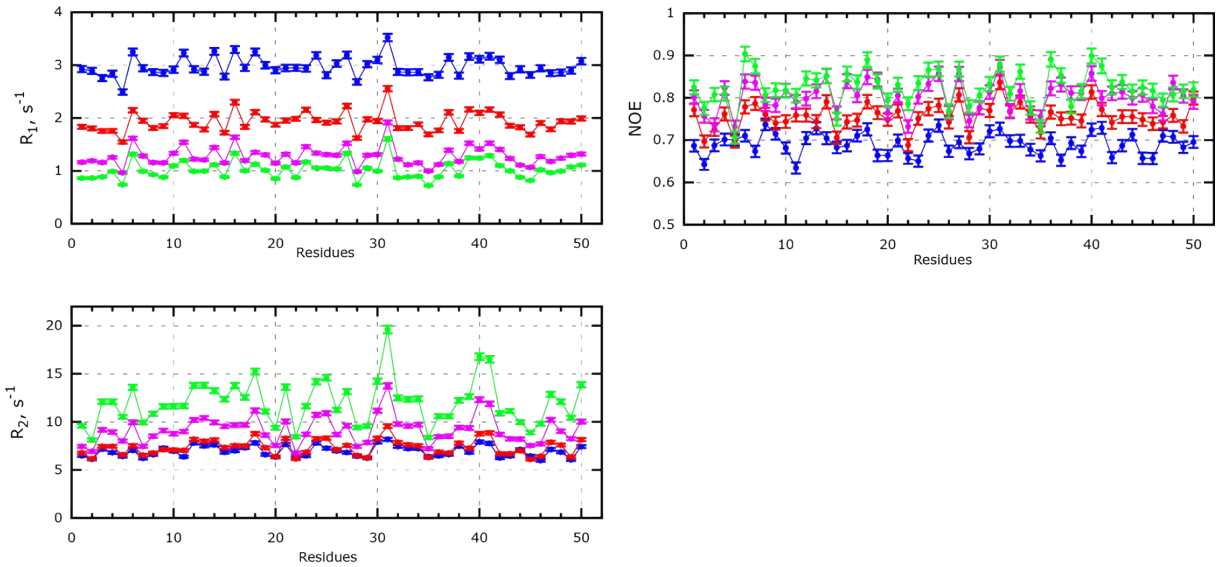

Figure S5: Representation of the calculated order parameters.

The S^2 are derived from the above relaxation parameters at each magnetic field: 9.4 (blue), 14.1 (red), 21.4 (violet) and 28.2 T (green) and by considering a uniform CSA value of -170 ppm. It is noteworthy to observe a large spread of S^2 for the highest magnetic field (green) when a constant value of CSA is used. The black line represents the values of S^2 fixed for the simulation.

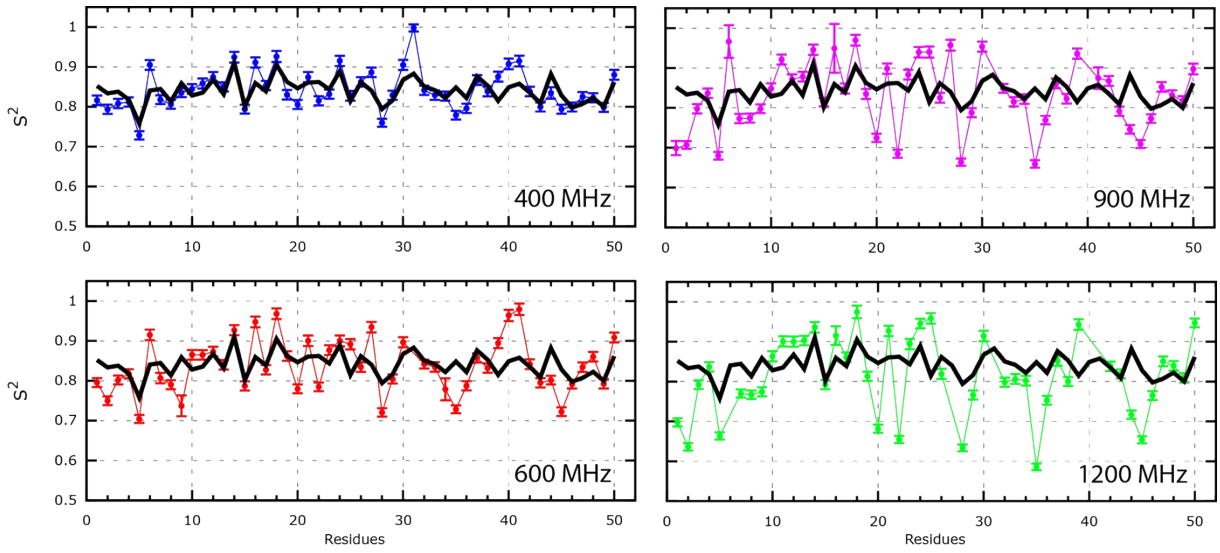

Figure S6: Fits of the dependence of $2R'_2 - R'_1$ on ω_N^2 for all considered residues in ubiquitin

The green lines are the least-squares fit lines with the logarithm robust method fit lines (see paragraph 3). The value of χ^2/df for the least-squares fit is given in the lower right corner of each panel. The 95% confidence level χ^2/df cutoff for this fit (which has 2 degrees of freedom for a typical data set here) is 2.99.


2 Δωre -160.31 ppm
χ²/df=0.20
3 Δωre -157.80 ppm
χ²/df=0.50
4 Δωre -148.55 ppm
χ²/df=0.37
5 Δωre -133.89 ppm
χ²/df=0.33
6 Δωre -155.99 ppm
χ²/df=0.41
7 Δωre -146.88 ppm
χ²/df=0.61
10 Δωre -190.05 ppm
χ²/df=0.31
11 Δωre -170.30 ppm
χ²/df=0.21
13 Δωre -195.45 ppm
χ²/df=0.07
14 Δωre -168.14 ppm
χ²/df=0.04
15 Δωre -151.92 ppm
χ²/df=1.12
16 Δωre -130.81 ppm
χ²/df=0.57
17 Δωre -157.62 ppm
χ²/df=0.09
18 Δωre -166.64 ppm
χ²/df=0.34
20 Δωre -157.69 ppm
χ²/df=0.03
21 Δωre -171.16 ppm
χ²/df=1.05
22 Δωre -196.22 ppm
χ²/df=0.32
26 Δωre -152.66 ppm
χ²/df=0.23
27 Δωre -165.18 ppm
χ²/df=0.59
28 Δωre -152.17 ppm
χ²/df=1.15
29 Δωre -149.95 ppm
χ²/df=0.32
30 Δωre -196.42 ppm
χ²/df=0.12
31 Δωre -166.01 ppm
χ²/df=0.75
32 Δωre -182.72 ppm
χ²/df=0.65
33 Δωre -164.73 ppm
χ²/df=0.65
34 Δωre -150.87 ppm
χ²/df=0.22
35 Δωre -173.62 ppm
χ²/df=0.73
36 Δωre -175.49 ppm
χ²/df=0.23
39 Δωre -159.99 ppm
χ²/df=0.07
40 Δωre -155.92 ppm
χ²/df=0.04
41 Δωre -158.44 ppm
χ²/df=0.01
42 Δωre -140.25 ppm
χ²/df=0.81
43 Δωre -142.83 ppm
χ²/df=1.10
44 Δωre -138.62 ppm
χ²/df=0.16
45 Δωre -194.77 ppm
χ²/df=0.59
47 Δωre -141.36 ppm
χ²/df=0.16
48 Δωre -160.96 ppm
χ²/df=0.39
49 Δωre -174.10 ppm
χ²/df=0.31
50 Δωre -160.41 ppm
χ²/df=0.08
51 Δωre -141.64 ppm
χ²/df=0.39
52 Δωre -148.55 ppm
χ²/df=0.27
54 Δωre -171.54 ppm
χ²/df=0.26
55 Δωre -184.40 ppm
χ²/df=0.36
56 Δωre -169.61 ppm
χ²/df=0.20
57 Δωre -149.42 ppm
χ²/df=0.07
58 Δωre -162.96 ppm
χ²/df=0.53
59 Δωre -156.64 ppm
χ²/df=0.32
60 Δωre -156.72 ppm
χ²/df=0.62
61 Δωre -196.17 ppm
χ²/df=0.38
62 Δωre -168.22 ppm
χ²/df=0.43
63 Δωre -134.58 ppm
χ²/df=0.61
64 Δωre -134.97 ppm
χ²/df=0.66
65 Δωre -162.52 ppm
χ²/df=0.30
66 Δωre -163.66 ppm
χ²/df=0.33
67 Δωre -153.07 ppm
χ²/df=0.09
68 Δωre -155.11 ppm
χ²/df=0.42
69 Δωre -170.55 ppm
χ²/df=0.18
70 Δωre -201.27 ppm
χ²/df=0.22
71 Δωre -160.97 ppm
χ²/df=0.62
72 Δωre -146.15 ppm
χ²/df=0.52
73 Δωre -150.24 ppm
χ²/df=0.55
74 Δωre -137.26 ppm
χ²/df=0.21

Table S1: Characteristics of the overall rotational diffusion tensor of ubiquitin.

The values are derived from ^{15}N relaxation data at different magnetic fields and assuming an axially symmetric tensor. Atom coordinates were taken from the NMR solution structure of ubiquitin (PDB entry 1D3Z).[1] Number in parentheses represent standard deviations.

Magnetic field (T)	$D_{\parallel}$[(a)] (10^7 s^{-1})	$D_{\perp}$[(a)] (10^7 s^{-1})	α (°)[(b)]	β (°)[(b)]	τ_C (ns)[(c)]	Anisotropy[(d)]	χ^2/df[(e)]
9.4	4.99 (0.45)	3.85 (0.29)	149 (23)	112 (23)	3.94 (0.06)	1.30 (0.39)	0.949
14.1	4.69 (0.33)	3.44 (0.25)	123 (35)	173 (20)	3.90 (0.06)	1.36 (0.29)	0.216
21.2	5.10 (0.08)	3.89 (0.05)	100 (8)	150 (4)	3.88 (0.01)	1.31 (0.04)	0.348
28.2	5.15 (0.08)	3.97 (0.05)	110 (9)	151 (3)	3.82 (0.01)	1.30 (0.04)	0.298

[(a)] Principal values of the axial rotational diffusion tensor
[(b)] Euler angles α,β describe the orientation of the diffusion tensor axis with respect to protein coordinate frame
[(c)] Overall rotational correlation time of the molecule
[(d)] The degree of anisotropy of the diffusion tensor
[(e)] Residuals of the fit divided by the number of degrees of freedom

Figure S7: Fitted dynamical parameters for ubiquitin from MD simulations.

Fitted parameters of the correlation function $C_I(t)$, to curves computed from molecular dynamics trajectories of ubiquitin for the AMBER ff99SB-ildn (a) and CHARMM36m (b) force fields. The three subplots respectively record the order parameters S^2, the set of motional parameters each containing a time-scale τ_j and a magnitude α_j, and the fast motions α_f that have timescales below the resolution of $C_I(t)$. All values are shaded according to the relative magnitude of contributions such that $S^2 + \sum_j \alpha_j + \alpha_f = 1$.

a) b)

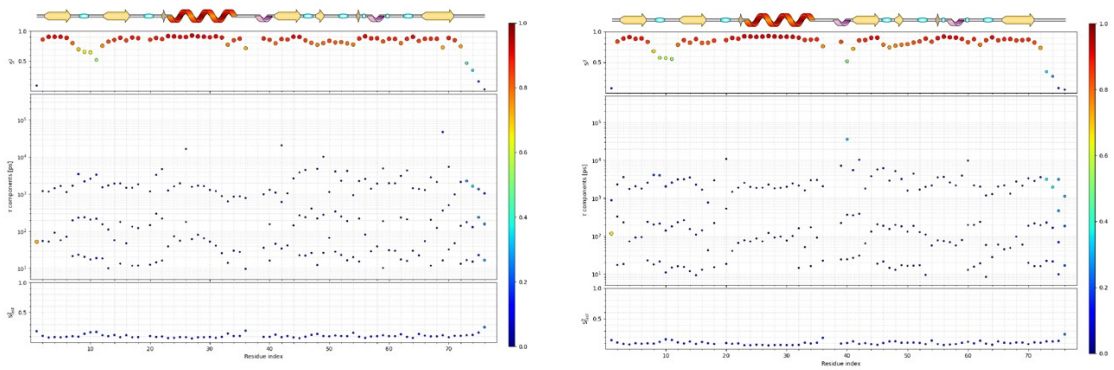

Figure S8: Computed NMR relaxation rates for ubiquitin with a 2 parameters fit for the AMBER force field.

Computed NMR relaxation of ubiquitin with χ^2-fitting of both D_{iso} and ζ at each magnetic field for the AMBER ff99SB-ildn force field. The blue, red, purple and green lines correspond to the experimental data at each magnetic fields while the black symbols correspond to the fitted data. Ile23 and Asn25 have been removed from analysis due to the presence of significant conformational exchange.

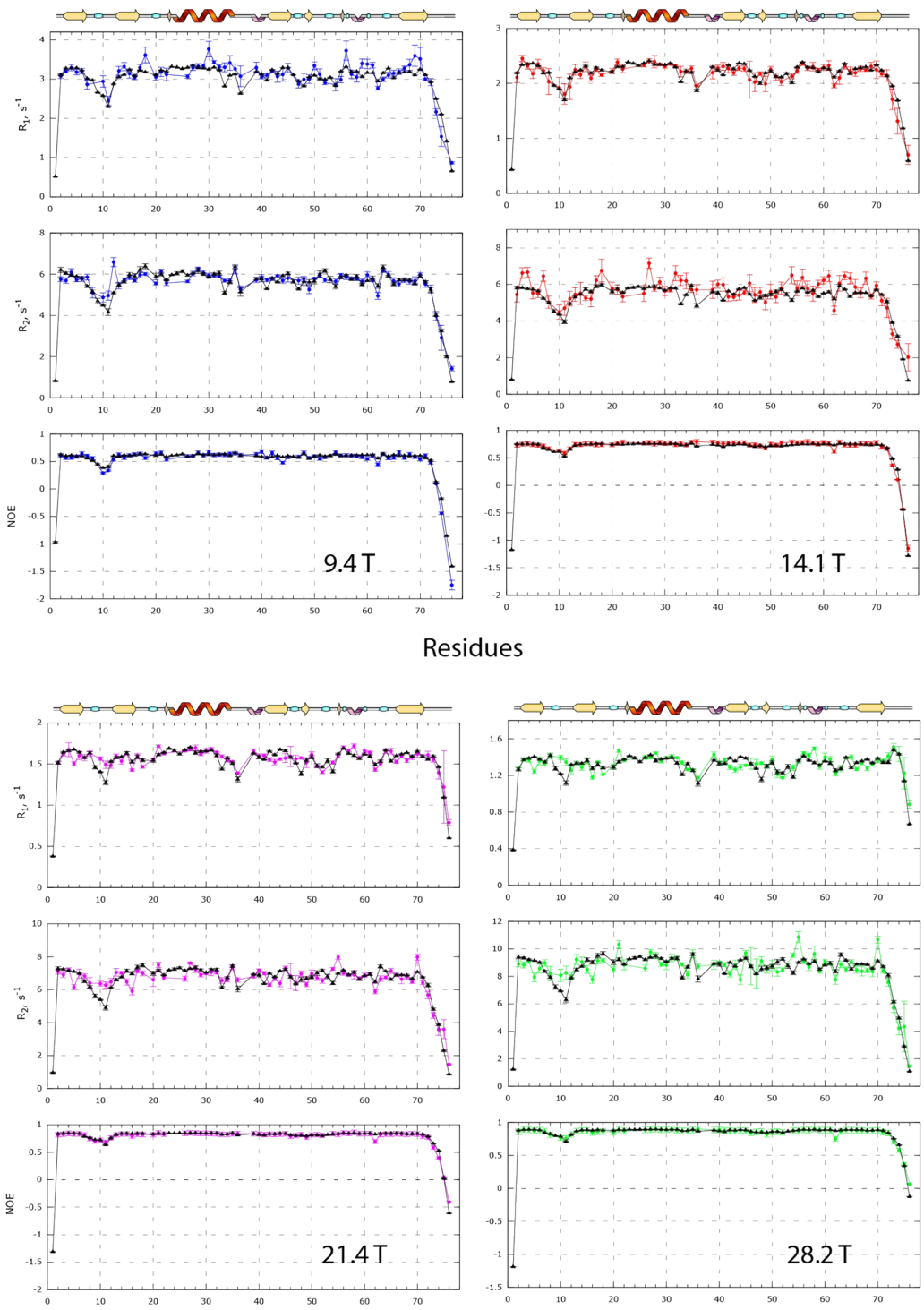

Figure S9: Computed NMR relaxation rates for ubiquitin with a 3 parameters fit for the AMBER force field.

Computed NMR relaxation of ubiquitin with χ^2-fitting of both D_{iso}, ζ and site-specific CSA at each magnetic field for the AMBER ff99SB-ildn force field. The blue, red, purple and green lines correspond to the experimental data at each magnetic fields while the black symbols correspond to the fitted data.

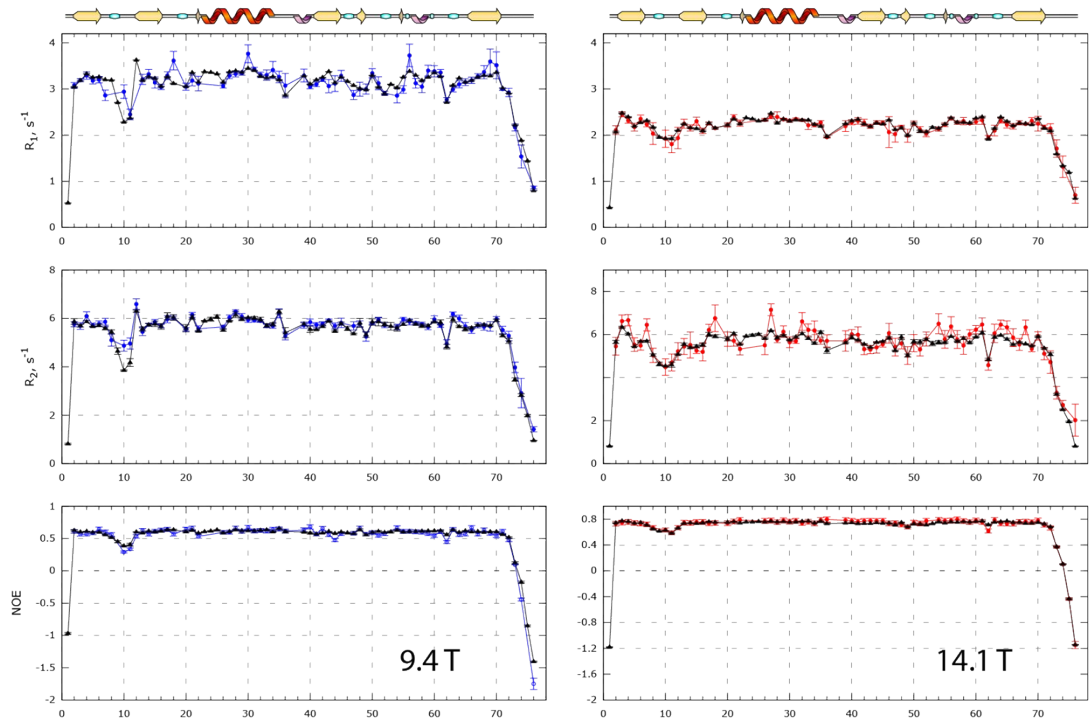

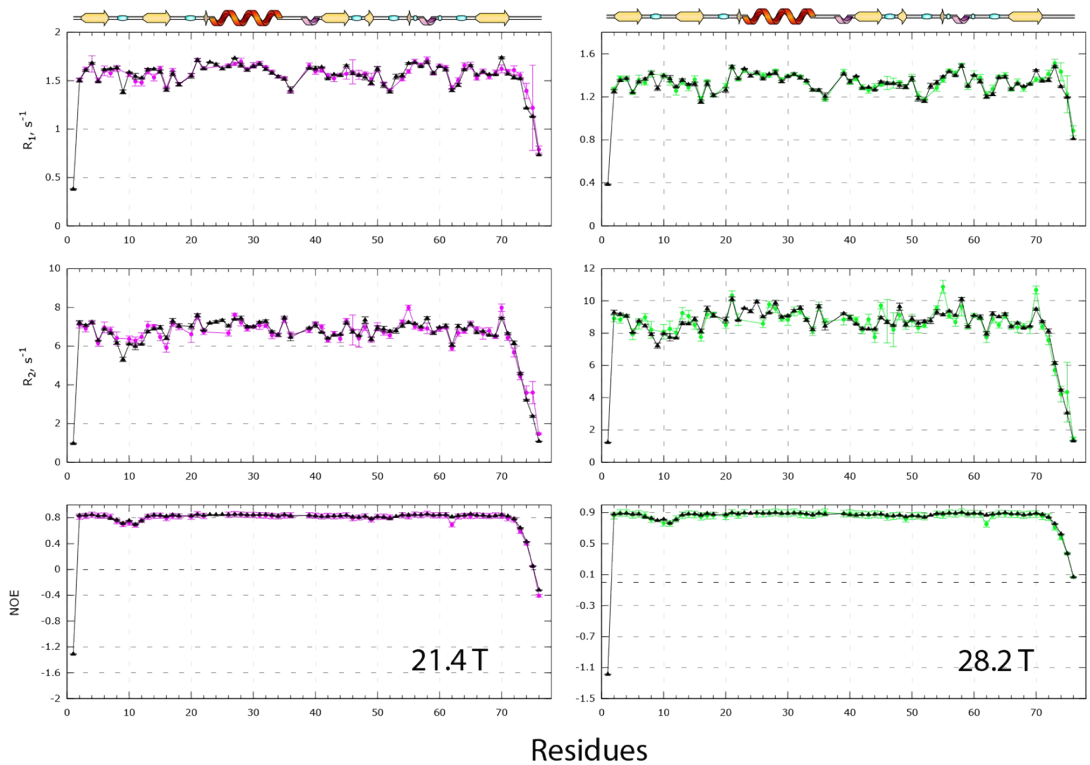

Figure S10: Computed NMR relaxation rates for ubiquitin with a 2 parameters fit for the CHARMM force field.

Computed NMR relaxation of ubiquitin with χ^2-fitting of both D_{iso} and ζ at each magnetic field for the CHARMM36m force field. The blue, red, purple and green lines correspond to the experimental data at each magnetic fields while the black symbols correspond to the fitted data.

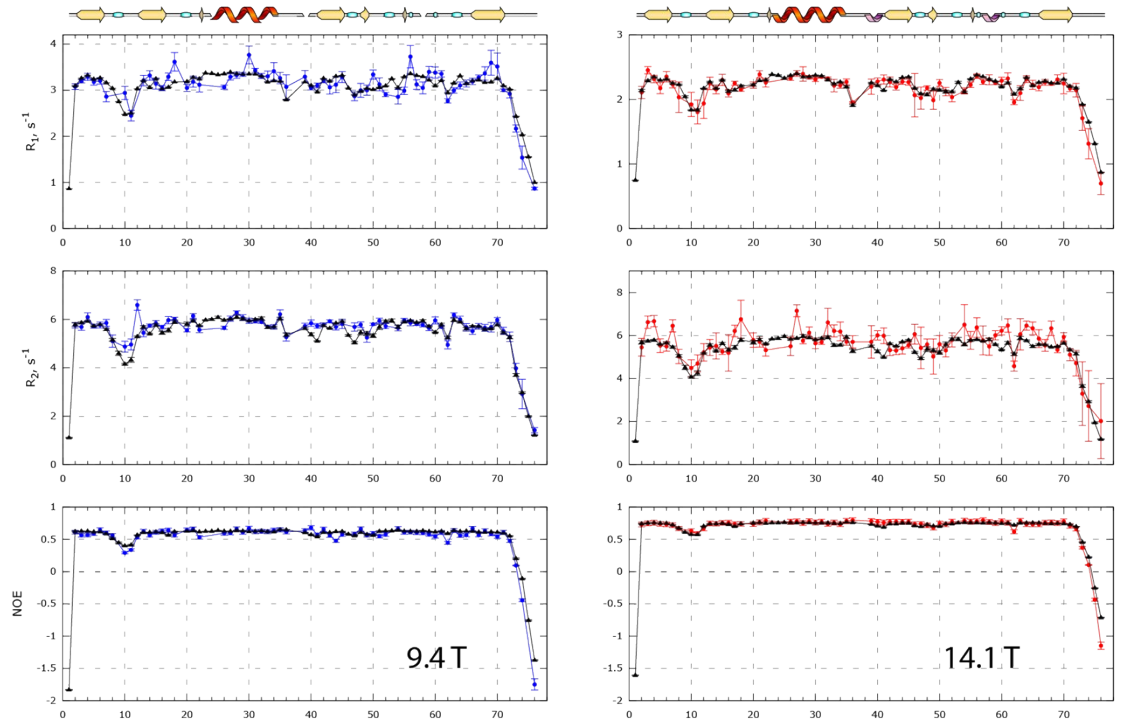

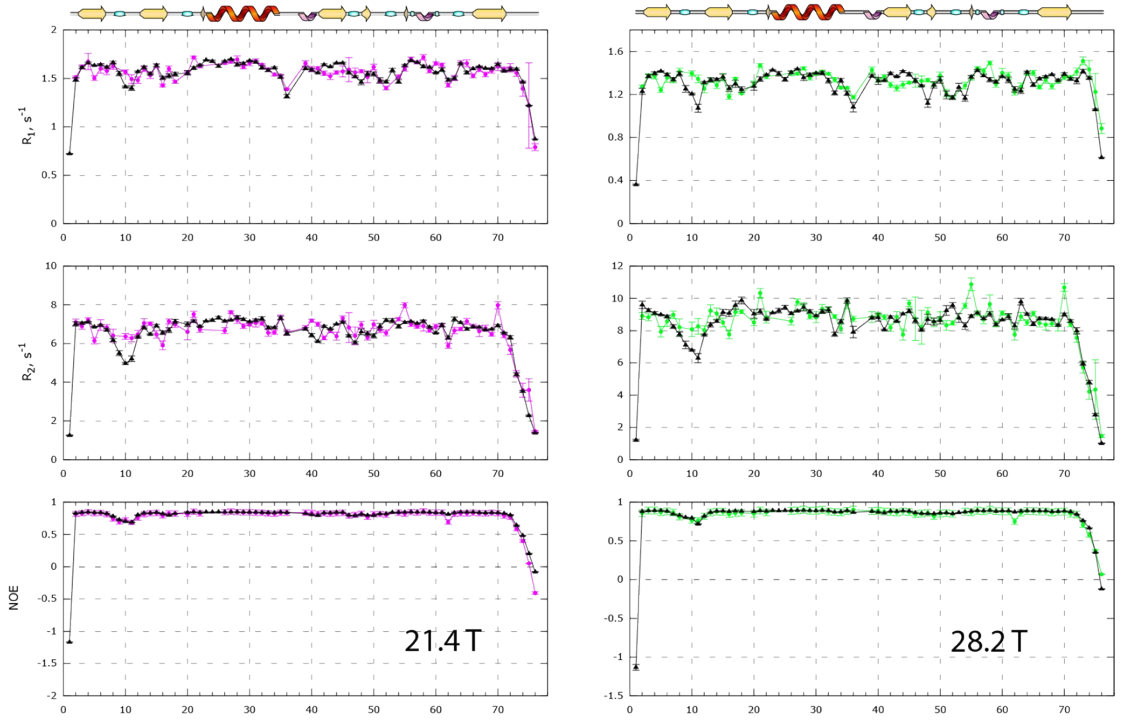

Figure S11: Computed NMR relaxation rates for ubiquitin with a 3 parameters fit for the CHARMM force field.

Computed NMR relaxation of ubiquitin with χ^2-fitting of both D_{iso}, ζ and site-specific CSA at each magnetic field for the CHARMM36m force field. The blue, red, purple and green lines correspond to the experimental data at each magnetic fields while the black symbols correspond to the fitted data.

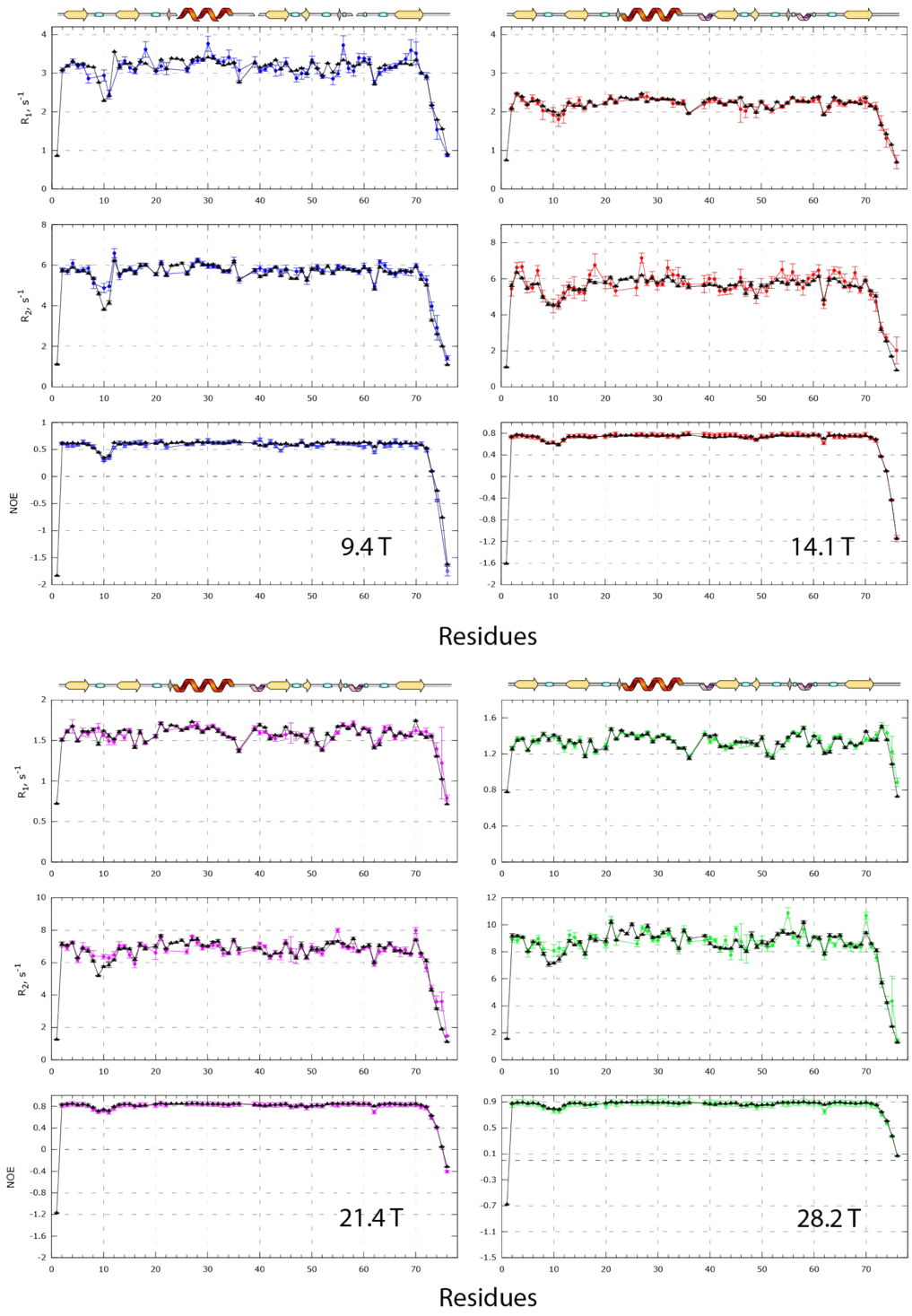

Figure S12: Relaxation parameters evolution as a function of the CSA for a given NH orientation.

Surface representation of the relaxation parameters as a function of the CSA value and the ^{1}H frequency for three distinct NH bond vectors orientation (left panel). The green arrow represents the orientation of the principal axis frame of diffusion while the blue arrow represents the NH vector orientation. The parameters used to calculate the different relaxation parameters are similar to the ones used in Fig. 1 (main text) and employ the analytical expression of eq.7. It is noticeable that the transverse relaxation rate is the most affected at very high magnetic field when the CSA value varies between -120 and -220 ppm.

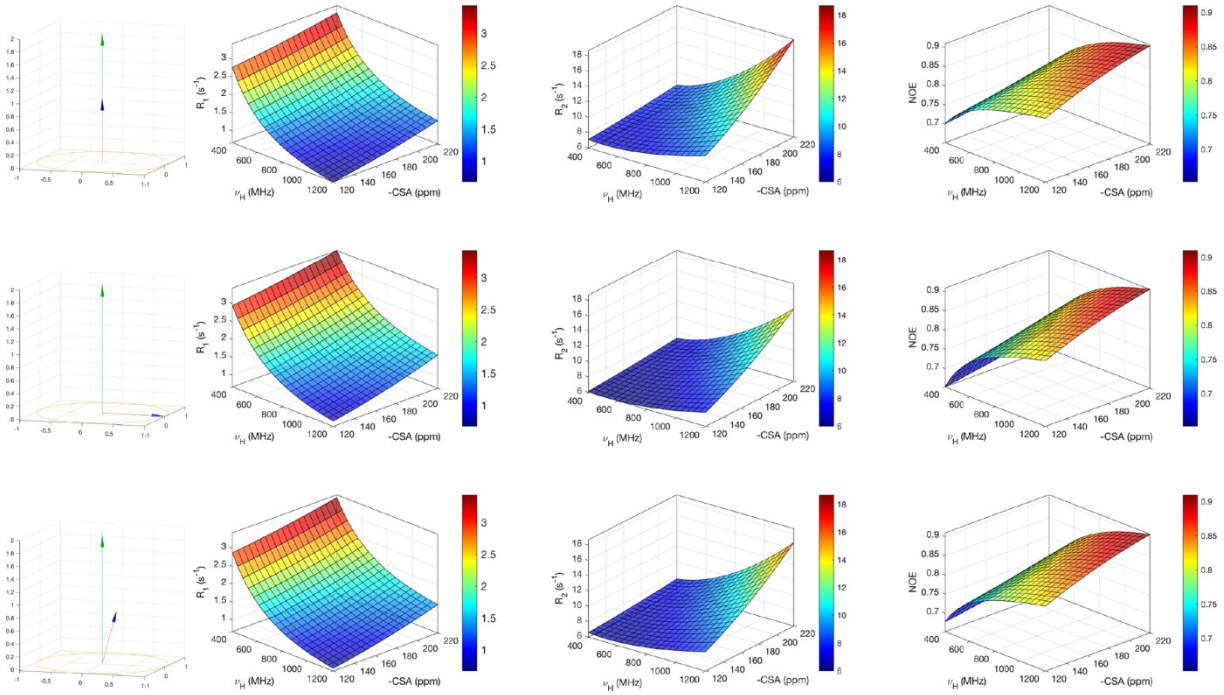

Figure S13: Computed NMR relaxation rates for GB3 with a 3 parameters fit for the AMBER force field.

Computed NMR relaxation of GB3 with χ^2-fitting of both D_{iso}, ζ and site-specific CSA at each magnetic field for the AMBER ff99SB-ildn force field. The black lines/symbols correspond to the fitted data while blue, purple, orange, green and red curves correspond to the experimental data at 9.4, 11.7, 14.1, 16.4 and 18.8 T respectively.

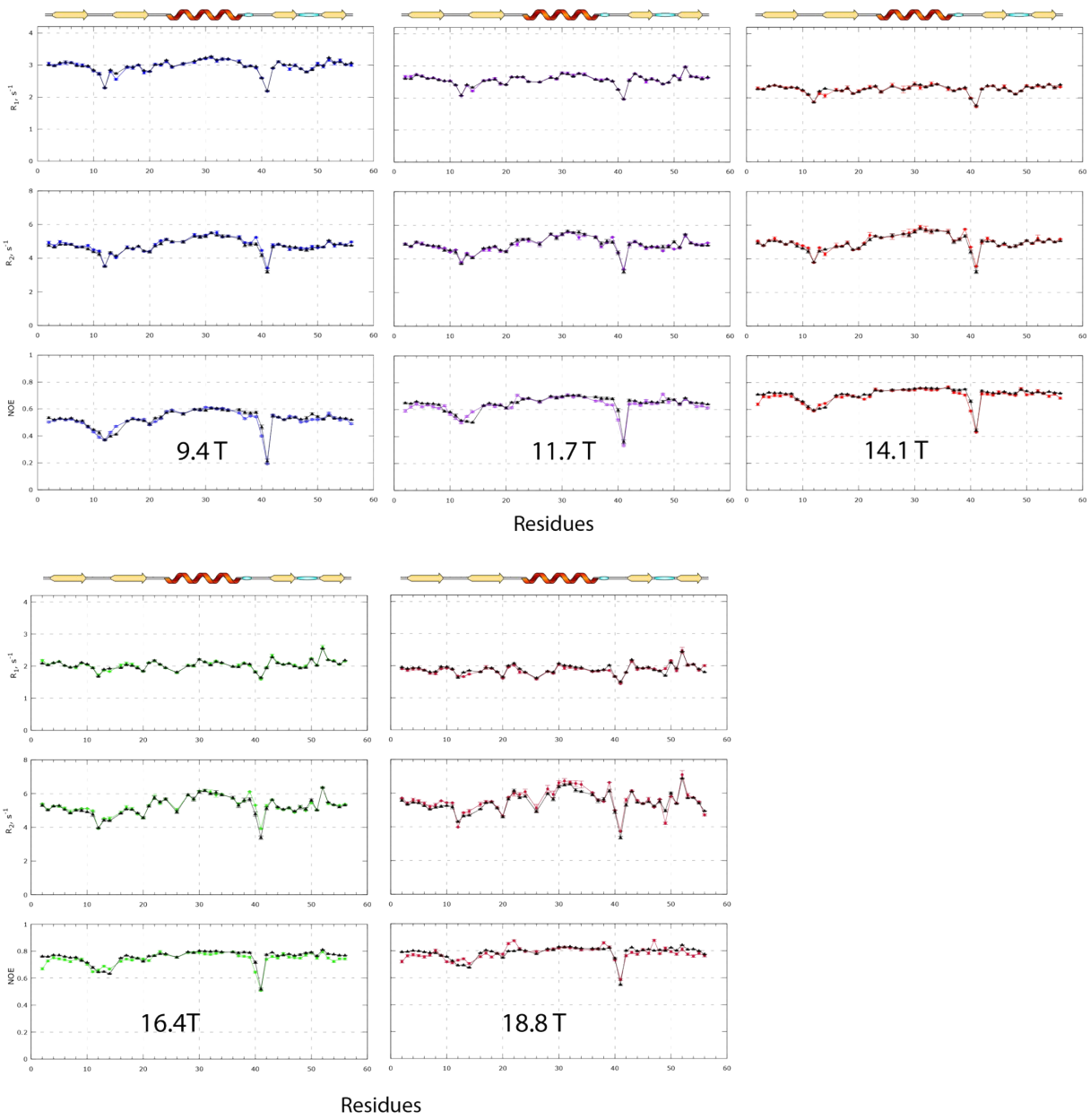

Figure S14: Computed NMR relaxation rates for GB3 with a 3 parameters fit for the CHARMM force field.

Computed NMR relaxation of GB3 with χ^2-fitting of both D_{iso}, ζ and site-specific CSA at each magnetic field for the CHARMM36m force field. The black lines/symbols correspond to the fitted data while blue, purple, orange, green and red curves correspond to the experimental data at 9.4, 11.7, 14.1, 16.4 and 18.8 T respectively.

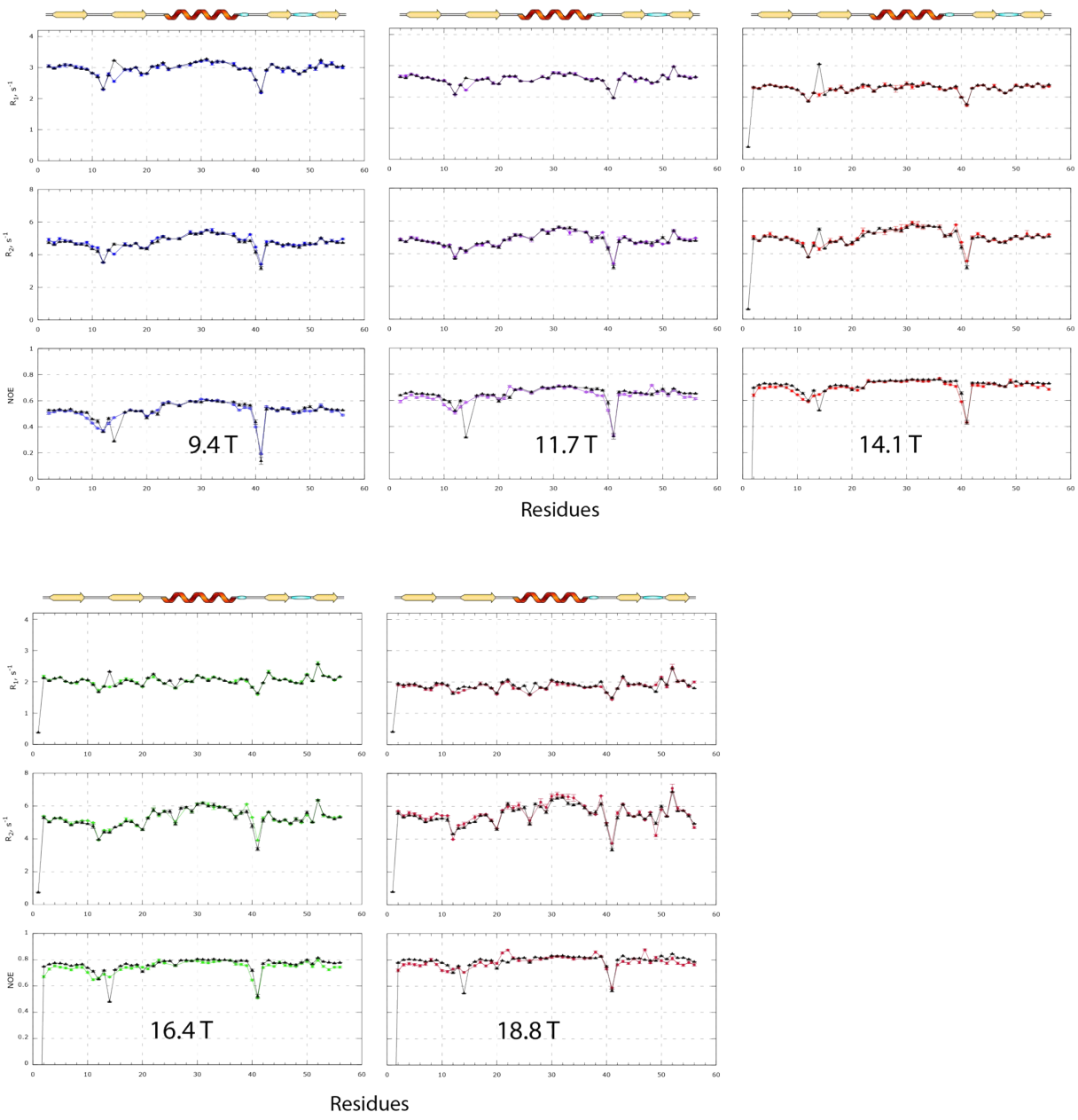

Figure S15: Fitted dynamical parameters for GB3.

Fitted parameters of the correlation function $C_I(t)$, to curves computed from molecular dynamics trajectories of GB3 for the AMBER ff99SB-ildn (a) and CHARMM36m (b) force fields. The three subplots respectively record the order parameters S^2, the set of motional parameters each containing a time-scale τ_j and a magnitude α_j, and the fast motions α_f that have timescales below the resolution of $C_I(t)$. All values are shaded according to the relative magnitude of contributions such that $S^2 + \sum_j \alpha_j + \alpha_f = 1$.

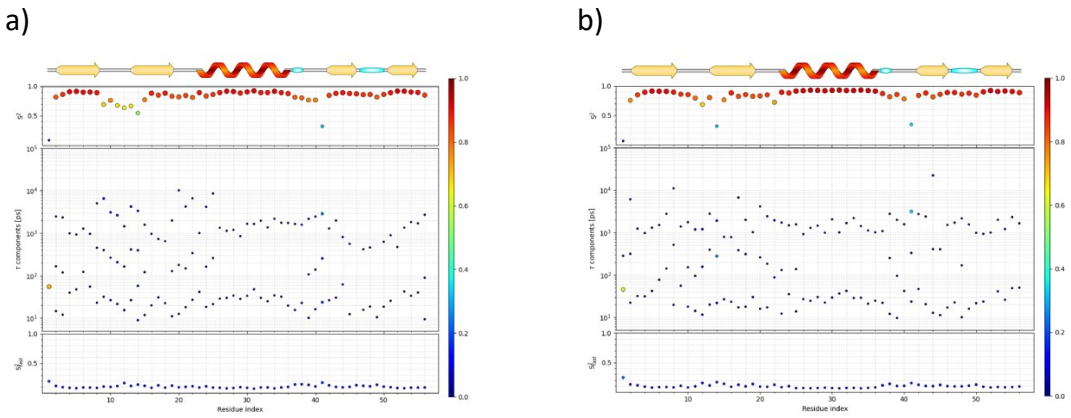

Figure S16: Fits of the dependence of $2R'_2 - R'_1$ on ω_N^2 for all considered residues in ribonuclease H.

The green lines are the least-squares fit lines with the logarithm robust method fit lines (see experimental methods). The red line represents a residue that did not pass the test. The value of χ^2/df for the least-squares fit is given in the lower right corner of each panel. The 95% confidence level χ^2/df cutoff for this fit (which has 2 degrees of freedom for a typical data set here) is 2.99. The relaxation data are taken from the published work of Kroenke *et al*.[2]

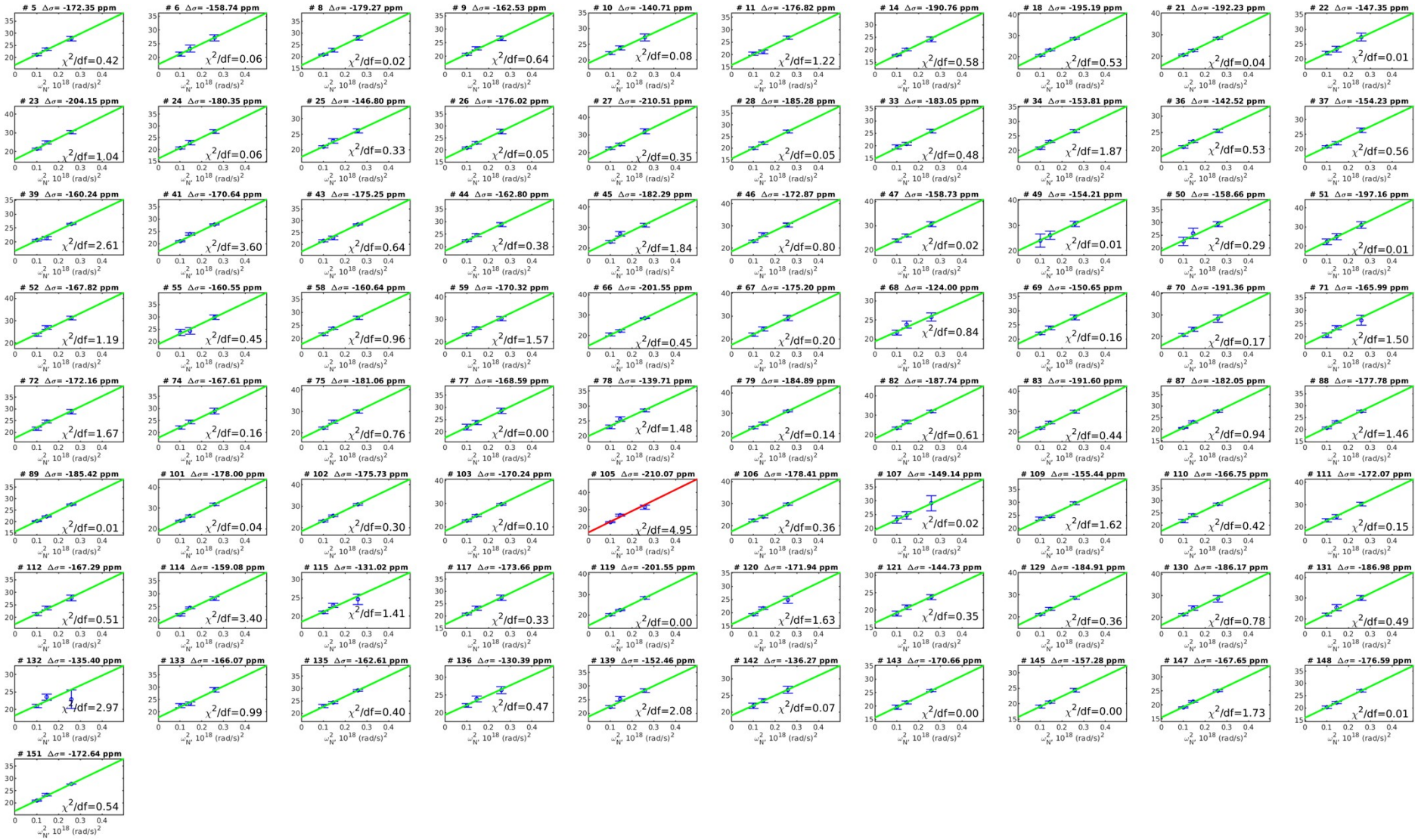
5 Δσ= -172.35 ppm
χ²/df=0.42
6 Δσ= -158.74 ppm
χ²/df=0.06
8 Δσ= -179.27 ppm
χ²/df=0.02
9 Δσ= -162.53 ppm
χ²/df=0.64
10 Δσ= -140.71 ppm
χ²/df=0.08
11 Δσ= -176.82 ppm
χ²/df=1.22
14 Δσ= -190.76 ppm
χ²/df=0.58
18 Δσ= -195.19 ppm
χ²/df=0.53
21 Δσ= -192.23 ppm
χ²/df=0.04
22 Δσ= -147.35 ppm
χ²/df=0.01
23 Δσ= -204.15 ppm
χ²/df=1.04
24 Δσ= -180.35 ppm
χ²/df=0.06
25 Δσ= -146.80 ppm
χ²/df=0.33
26 Δσ= -176.02 ppm
χ²/df=0.05
27 Δσ= -210.51 ppm
χ²/df=0.35
28 Δσ= -185.28 ppm
χ²/df=0.05
33 Δσ= -183.05 ppm
χ²/df=0.48
34 Δσ= -153.81 ppm
χ²/df=1.87
36 Δσ= -142.52 ppm
χ²/df=0.53
37 Δσ= -154.23 ppm
χ²/df=0.56
39 Δσ= -160.24 ppm
χ²/df=2.61
41 Δσ= -170.64 ppm
χ²/df=3.60
43 Δσ= -175.25 ppm
χ²/df=0.64
44 Δσ= -162.80 ppm
χ²/df=0.38
45 Δσ= -182.29 ppm
χ²/df=1.84
46 Δσ= -172.87 ppm
χ²/df=0.80
47 Δσ= -158.73 ppm
χ²/df=0.02
49 Δσ= -154.21 ppm
χ²/df=0.01
50 Δσ= -158.66 ppm
χ²/df=0.29
51 Δσ= -197.16 ppm
χ²/df=0.01
52 Δσ= -167.82 ppm
χ²/df=1.19
55 Δσ= -160.55 ppm
χ²/df=0.45
58 Δσ= -160.64 ppm
χ²/df=0.96
59 Δσ= -170.32 ppm
χ²/df=1.57
66 Δσ= -201.55 ppm
χ²/df=0.45
67 Δσ= -175.20 ppm
χ²/df=0.20
68 Δσ= -124.00 ppm
χ²/df=0.84
69 Δσ= -150.65 ppm
χ²/df=0.16
70 Δσ= -191.36 ppm
χ²/df=0.17
71 Δσ= -165.99 ppm
χ²/df=1.50
72 Δσ= -172.16 ppm
χ²/df=1.67
74 Δσ= -167.61 ppm
χ²/df=0.16
75 Δσ= -181.06 ppm
χ²/df=0.76
77 Δσ= -168.59 ppm
χ²/df=0.00
78 Δσ= -139.71 ppm
χ²/df=1.48
79 Δσ= -184.89 ppm
χ²/df=0.14
82 Δσ= -187.74 ppm
χ²/df=0.61
83 Δσ= -191.60 ppm
χ²/df=0.44
87 Δσ= -182.05 ppm
χ²/df=0.94
88 Δσ= -177.78 ppm
χ²/df=1.46
89 Δσ= -185.42 ppm
χ²/df=0.01
101 Δσ= -178.00 ppm
χ²/df=0.04
102 Δσ= -175.73 ppm
χ²/df=0.30
103 Δσ= -170.24 ppm
χ²/df=0.10
105 Δσ= -210.07 ppm
χ²/df=4.95
106 Δσ= -178.41 ppm
χ²/df=0.36
107 Δσ= -149.14 ppm
χ²/df=0.02
109 Δσ= -155.44 ppm
χ²/df=1.62
110 Δσ= -166.75 ppm
χ²/df=0.42
111 Δσ= -172.07 ppm
χ²/df=0.15
112 Δσ= -167.29 ppm
χ²/df=0.51
114 Δσ= -159.08 ppm
χ²/df=3.40
115 Δσ= -131.02 ppm
χ²/df=1.41
117 Δσ= -173.66 ppm
χ²/df=0.33
119 Δσ= -201.55 ppm
χ²/df=0.00
120 Δσ= -171.94 ppm
χ²/df=1.63
121 Δσ= -144.73 ppm
χ²/df=0.35
129 Δσ= -184.91 ppm
χ²/df=0.36
130 Δσ= -186.17 ppm
χ²/df=0.78
131 Δσ= -186.98 ppm
χ²/df=0.49
132 Δσ= -135.40 ppm
χ²/df=2.97
133 Δσ= -166.07 ppm
χ²/df=0.99
135 Δσ= -162.61 ppm
χ²/df=0.40
136 Δσ= -130.39 ppm
χ²/df=0.47
139 Δσ= -152.46 ppm
χ²/df=2.08
142 Δσ= -136.27 ppm
χ²/df=0.07
143 Δσ= -170.66 ppm
χ²/df=0.00
145 Δσ= -157.28 ppm
χ²/df=0.00
147 Δσ= -167.65 ppm
χ²/df=1.73
148 Δσ= -176.59 ppm
χ²/df=0.01
151 Δσ= -172.64 ppm
χ²/df=0.54
ω²N, 10¹⁸ (rad/s)²

Figure S17: Deduced Δσ and S^2 for a uniform and site-specific CSA for ribonuclease H.

(a) Values of Δσ deduced from the $2R'_2$-R'_1 method for ribonuclease H. The red dashed line represents the average value of Δσ. (b) Backbone order parameters derived from a LS analysis of the ^{15}N relaxation data (R_1, R_2, NOE) from Kroenke *et al.*[2] at different fields assuming a uniform CSA of -160 ppm. (c) Backbone order parameters derived from a LS analysis of the ^{15}N relaxation data (R_1, R_2, NOE) at different fields assuming experimental site-specific ^{15}N CSA. The thickness of the curves in (b) and (c) reflects the error on S^2 for each residue.

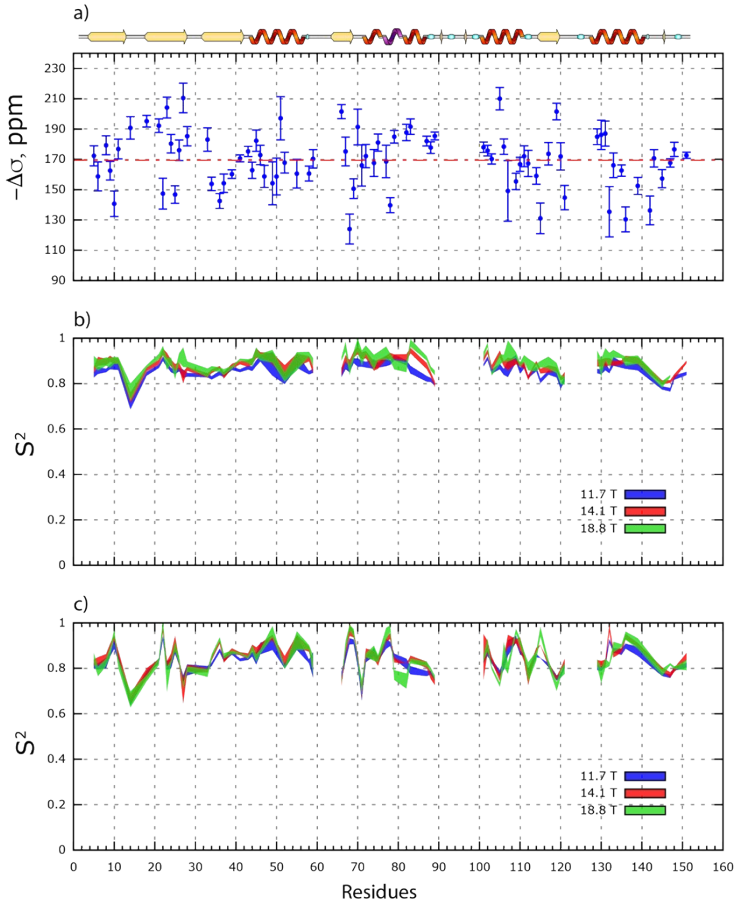

Table S2: Characteristics of the overall rotational diffusion tensor of ribonuclease H.

Characteristics of the overall rotational diffusion tensor of ribonuclease H derived from ^{15}N relaxation data at different magnetic fields and assuming an axially symmetric tensor. Atom coordinates were taken from the NMR solution structure of ribonuclease H (PDB entry 1RNH).[3]

Magnetic field (T)	$D_{\parallel}$[(a)] (10^7 s^{-1})	$D_{\perp}$[(a)] (10^7 s^{-1})	α (°)[(b)]	β (°)[(b)]	τ_C (ns)[(c)]	Anisotropy[(d)]	χ^2/df[(e)]
11.8	1.98 (0.02)	1.55 (0.01)	69 (3)	84 (2)	9.86 (0.02)	1.28 (0.02)	0.316
14.1	1.95 (0.02)	1.57 (0.01)	58 (3)	89 (2)	9.82 (0.02)	1.24 (0.02)	0.355
18.8	2.00 (0.04)	1.61 (0.02)	55 (13)	89 (4)	9.58 (0.03)	1.24 (0.07)	0.332

[(a)] Principal values of the axial rotational diffusion tensor
[(b)] Euler angles α,β describe the orientation of the diffusion tensor axis with respect to protein coordinate frame
[(c)] Overall rotational correlation time of the molecule
[(d)] The degree of anisotropy of the diffusion tensor
[(e)] Residuals of the fit divided by the number of degrees of freedom

Figure S18: Fitted dynamical parameters for ribonuclease H.

Fitted parameters of the correlation function $C_I(t)$, to curves computed from molecular dynamics trajectories of ribonuclease H for the AMBER ff99SB-ildn (a) and CHARMM36m (b) force fields. The three subplots respectively record the order parameters S^2, the set of motional parameters each containing a time-scale τ_j and a magnitude α_j, and the fast motions α_f that have timescales below the resolution of $C_I(t)$. All values are shaded according to the relative magnitude of contributions such that $S^2 + \sum_j \alpha_j + \alpha_f = 1$.

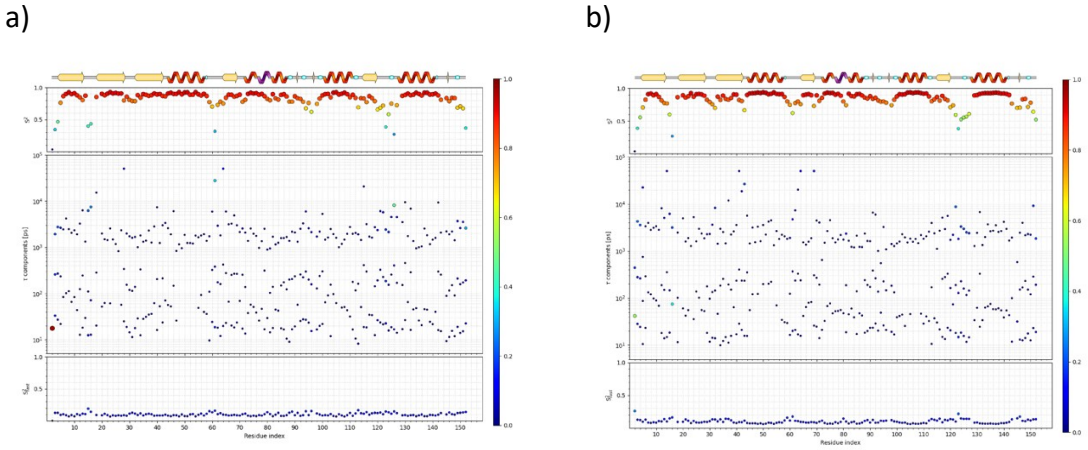

Figure S19: Computed NMR relaxation rates for ribonuclease H with a 3 parameters fit for the AMBER force field.

Computed NMR relaxation of ribonuclease H with χ^2-fitting of both D_{iso}, ζ and site-specific CSA at each magnetic field for the AMBER ff99SB-ildn force field. The black lines correspond to the fitted data while blue, red and green curves correspond to the experimental data at 11.7, 14.1 and 18.8 T respectively.

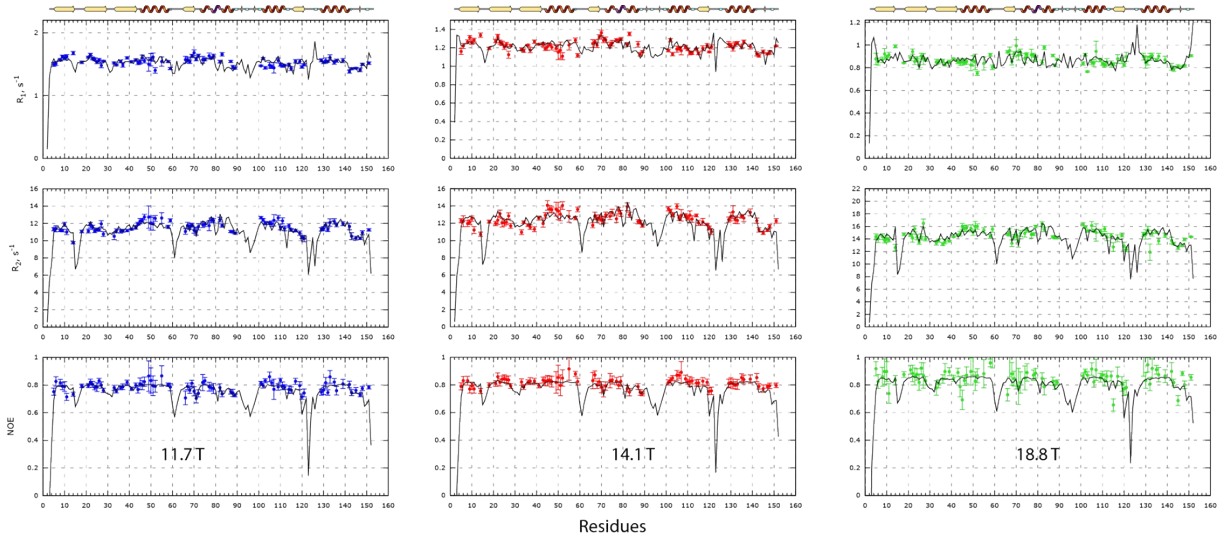

Figure S20: Computed NMR relaxation rates for ribonuclease H with a 3 parameters fit for the CHARMM force field.

Computed NMR relaxation of ribonuclease H with χ^2-fitting of both D_{iso}, ζ and site-specific CSA at each magnetic field for the CHARMM36m force field. The black lines correspond to the fitted data while blue, red and green curves correspond to the experimental data at 11.7, 14.1 and 18.8 T respectively.

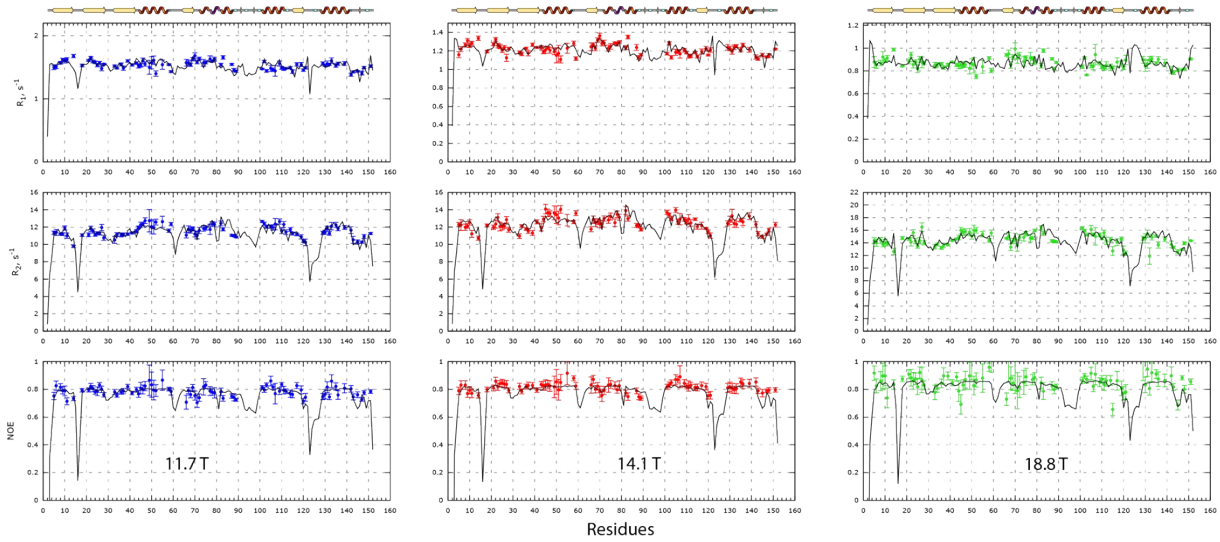

Figure S21: Computed NMR relaxation rates of ubiquitin with 3 parameters at 28.2 T.

Computed NMR relaxation of ubiquitin with χ^2-fitting of both D_{iso}, ζ and site-specific CSA for a magnetic field of 28.2 T. The green line corresponds to the experimental data while the black

symbols correspond to the fitted data. It is noticeable that our fitting procedure allows the identification of Ile23 and Asn25 as residues affected by conformational exchange.

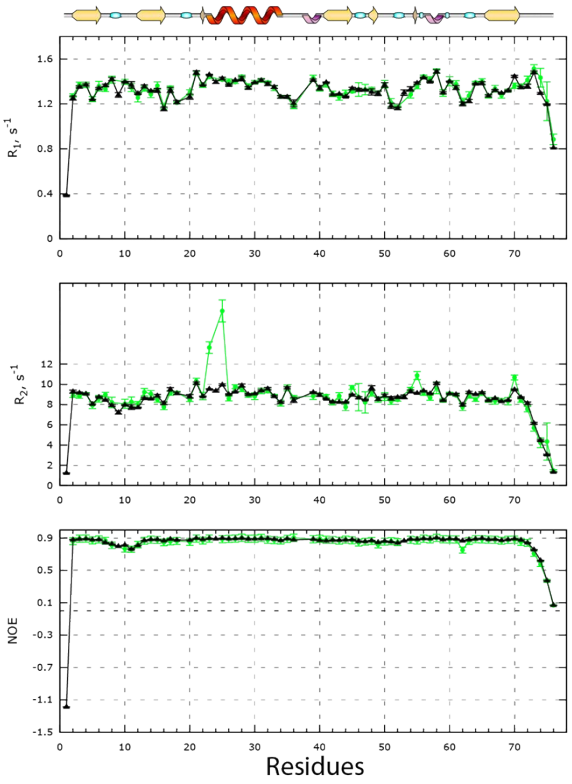

References:

1. Cornilescu, G.; Marquardt, J. L.; Ottiger, M.; Bax, A., Validation of Protein Structure from Anisotropic Carbonyl Chemical Shifts in a Dilute Liquid Crystalline Phase. *J. Am. Chem. Soc* **1998,** *120*, 6836-6837.
2. Kroenke, C. D.; Rance, M.; Palmer, A. G., Variability of the 15N Chemical Shift Anisotropy in Escherichia coli Ribonuclease H in Solution. *J Am Chem Soc* **1999,** *121* (43), 10119-10125.
3. Yang, W.; Hendrickson, W. A.; Crouch, R. J.; Satow, Y., Structure of Ribonuclease H Phased at 2 Å Resolution by MAD Analysis of the Selenomethionyl Protein. *Science* **1990,** *249* (4975), 1398-1405.